

Extraction of the defect density of states in microcrystalline silicon from experimental results and simulation studies

T. Tibermacine^{1,†}, A. Merazga², M. Ledra¹, and N. Ouhabab¹

¹Laboratory of Metallic and Semi-conducting Materials, University of Biskra, Biskra 07000, Algeria

²Physics Department, Faculty of Science, Taif University, Al-Hawia, Taif, Saudi Arabia

Abstract: The constant photocurrent method in the ac-mode (ac-CPM) is used to determine the defect density of states (DOS) in hydrogenated microcrystalline silicon ($\mu\text{c-Si:H}$) prepared by very high frequency plasma-enhanced chemical vapor deposition (VHF-PECVD). The absorption coefficient spectrum ($\text{ac-}\alpha(h\nu)$), is measured under ac-CPM conditions at 60 Hz. The measured $\text{ac-}\alpha(h\nu)$ is converted by the CPM spectroscopy into a DOS distribution covering a portion in the lower energy range of occupied states. We have found that the density of valence band-tail states falls exponentially towards the gap with a typical band-tail width of 63 meV. Independently, computer simulations of the ac-CPM are developed using a DOS model that is consistent with the measured $\text{ac-}\alpha(h\nu)$ in the present work and a previously measured transient photocurrent (TPC) for the same material. The DOS distribution model suggested by the measurements in the lower and in the upper part of the energy-gap, as well as by the numerical modelling in the middle part of the energy-gap, coincide reasonably well with the real DOS distribution in hydrogenated microcrystalline silicon because the computed $\text{ac-}\alpha(h\nu)$ is found to agree satisfactorily with the measured $\text{ac-}\alpha(h\nu)$.

Key words: constant photocurrent method; optical absorption spectrum; micro-crystalline silicon; defect density of states

DOI: 10.1088/1674-4926/36/9/093001

EEACC: 2520

1. Introduction

Recently, hydrogenated microcrystalline silicon ($\mu\text{c-Si:H}$) has attracted considerable interest for use in optoelectronic applications. As compared to hydrogenated amorphous silicon (a-Si:H), it offers a higher stability against light degradation and a wider absorption bandwidth that extends into the near infrared. The electronic properties and performance of hydrogenated microcrystalline silicon ($\mu\text{c-Si:H}$) films are correlated with the deposition parameters and the structural properties^[1–3]. It is in fact heterogeneous in nature, which leads to difficulties in explaining its electronic transport properties. Therefore, the detailed knowledge of the density of states (DOS) in $\mu\text{c-Si:H}$ is of great importance to understand the transport mechanism. However, since $\mu\text{c-Si:H}$ is a phase mixture of crystalline and amorphous regions separated by grain boundaries and voids, little is known about the nature and the energy distribution of the DOS. It is, therefore, not surprising if there is no conclusive DOS map. Sub-band gap absorption spectroscopy, such as the constant photocurrent method (CPM)^[4–6], photo-thermal deflection spectroscopy (PDS)^[5, 7] and dual beam photoconductivity (DBP)^[8], have been used to determine the DOS in the lower energy range of the band gap near the valence band, whereas the transient photoconductivity (TPC) has been used to determine the DOS in the upper energy range of the gap, close to the conduction band. On the simulation side, great effort was deployed to model the TPC in $\mu\text{c-Si:H}$ ^[9], while modeling has been less employed to elucidate the experimental results of the CPM technique in $\mu\text{c-Si:H}$, particularly in the ac mode.

In the present work, we have used the constant photocurrent method in the ac-mode (ac-CPM) to measure the absorption coefficient spectrum ($\text{ac-}\alpha(h\nu)$) in very high frequency plasma-enhanced chemical vapor deposition (VHF-PECVD) prepared $\mu\text{c-Si:H}$ and we have applied the derivative method of Pierz *et al.*^[10] to convert the measured data into a DOS distribution in the lower part of the energy-gap. We have completed the $\mu\text{c-Si:H}$ DOS model in the upper part of the energy-gap and around the mid-gap by using previous DOS data based on transient photocurrent (TPC) spectroscopy^[11], and by a Si:H-like dangling bond defect DOS with appropriate parameters from References [12–15], respectively. On the basis of this complete DOS model, we have developed numerical simulations of the ac-CPM, taking into account both carrier types in the absorption and transport processes.

2. Theory

Photocurrent techniques detect optically induced transitions between localised levels in the band-gap and extended levels in the bands, which generates free carriers. This should allow us to determine, by appropriate spectroscopy methods, the density and energy position of the defect states within the forbidden optical gap. The CPM was introduced by Vanecek *et al.*^[5]. The basic idea of the CPM is to adjust the photon flux so that photoconductivity remains constant throughout the sample for all of the incident photon energies. Under these conditions, one ensures that the occupation of the electronic states is constant, as well as the concentration of the photo-generated carriers. Under these circumstances, the $\mu\tau$ product remains

[†] Corresponding author. Email: tawfik_tiber@yahoo.fr

Received 19 January 2015, revised manuscript received 17 April 2015

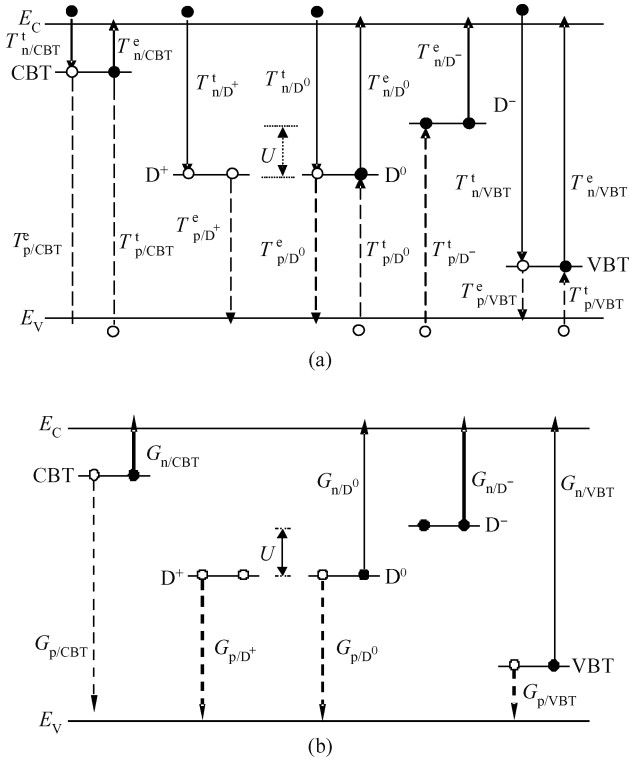


Figure 1. (a) Thermal and (b) optical carrier transitions involved in the CPM simulation.

constant for all of the used wavelengths. However, when the photocurrent is kept constant for all of the monochromatic photon energies $h\nu$, the carrier lifetime is, in good approximation, also constant. Furthermore, the mobility μ assumed to be constant. The resulting absorption coefficient is dependent only on the incident photon flux and is given by:

$$\alpha(h\nu)\phi_{ph}(h\nu) = C, \quad \Leftrightarrow \alpha(h\nu) \propto \frac{1}{\phi_{ph}(h\nu)}, \quad (1)$$

where C is an energy independent constant. This constant, and $\alpha(h\nu)$, are calibrated with the absolute absorption coefficient obtained from reflection/transmission measurements^[16].

3. Numerical modelling

Figure 1 illustrates the thermal and optical carrier transitions for the CPM for a uniform sub-gap illumination. While single level representation appears in the illustration, the DOS components CT, VT, D^0 , D^- and D^+ are energetically-distributed. At room temperature, photoconduction is carried out by free carriers, and so the only transitions taken into account are those between localised states in the gap and extended states in the bands. In addition, because of their small probabilities, band-to-band transitions are ignored.

The thermal transition rates T have the following significance:

$T_{n(p)/CBT(VBT)}^{t(e)}$ (E): Rates of electron (hole) trapping (emission) into (from) a level E at the conduction band tail (valence band tail).

$T_{n/D^0(D^+)}^t$ (E): Rates of electron trapping into a D^0 (D^+) level E at the defect states distribution.

$T_{n/D^0(D^-)}^e$ (E): Rates of electron emission from a D^0 (D^-) level E at the defect states distribution.

$T_{p/D^0(D^-)}^t$ (E): Rates of hole trapping into a D^0 (D^-) level E at the defect states distribution.

$T_{p/D^0(D^+)}^e$ (E): Rates of hole emission from a D^0 (D^+) level E at the defect states distribution.

The trapping rate is a function of free $n(p)$ and trapped $n_t(p_t)$ carrier densities following this relation:

$$T_{n(p)}^t(E) = C_{n(p)}n(p)[D_t(E) - n_t(p_t)], \quad (2)$$

where $D_t(E)$ is the total DOS at level E and $C_{n(p)}$ is the capture coefficient of the trapping state. Similarly, the emission rate is a function of trapped $n_t(p_t)$ carrier densities following the relation:

$$T_{n(p)}^e(E) = C_{n(p)}D_{CB(VB)}n_t(p_t) \times \exp(-|E - E_{CB(VB)}|/(k_B T)), \quad (3)$$

where $D_{CB(VB)}$ is the effective DOS at the conduction (valence) mobility edge $E_{CB(VB)}$ (k_B is Boltzmann constant and T the temperature). The optical generation rates G have the following significance:

(1) $G_{n(p)/VBT(CBT)}$ (E): Rates of electron (hole) generation from a level E at the valence band tail (conduction band tail).

(2) $G_{n/D^0(D^-)}$ (E): Rates of electron generation from a D^0 (D^-) level E at the defect states distribution.

(3) $G_{p/D^0(D^+)}$ (E): Rates of hole generation from a D^0 (D^+) level E at the defect states distribution.

The optical generation rate is a function of the free and trapped carrier densities, following the equation:

$$G_{n(p)}(E, h\nu) = \phi_{ph} \frac{K}{h\nu} [D_{CB(VB)} - n(p)]n_t(D_t)(E), \quad (4)$$

where $K = 4.34 \times 10^{-38} \text{ cm}^5 \cdot \text{eV}^2$ is a constant proportional to the momentum matrix element. We restrict our simulations to the ac-CPM, where the carriers are created by chopped optical illumination of photon energy $h\nu$ lower than the material energy-gap, and consider the case of a small signal. With reference to Figure 1, the well known rate equations which control the photo-transport under any static or dynamic photo-excitation regime^[17] requires transferring to the frequency domain using the Fourier integral in the case of ac-CPM. To solve the ac-CPM equations, we divide the energy gap into N closely spaced energy levels E_i , including the band edges $E_V = E_1$ and $E_C = E_N$, so that the total number of equations to solve for the same number of variable densities (\hat{n} , \hat{p} , \hat{n}_{ti} , \hat{p}_{ti} , \hat{D}^0 , \hat{D}^+ and \hat{D}^-) is $4N - 2$.

In modelling coplanar samples, it is common practice to assume a uniform electric field, perfect Ohmic contacts, and to neglect any transport driven by free-carrier diffusion. Under these assumptions, the continuity equation for holes is automatically satisfied when the continuity equation for electrons and the charge neutrality condition are fulfilled. We have developed a computer code to solve the system of equations using appropriate numerical techniques. As required by the CPM

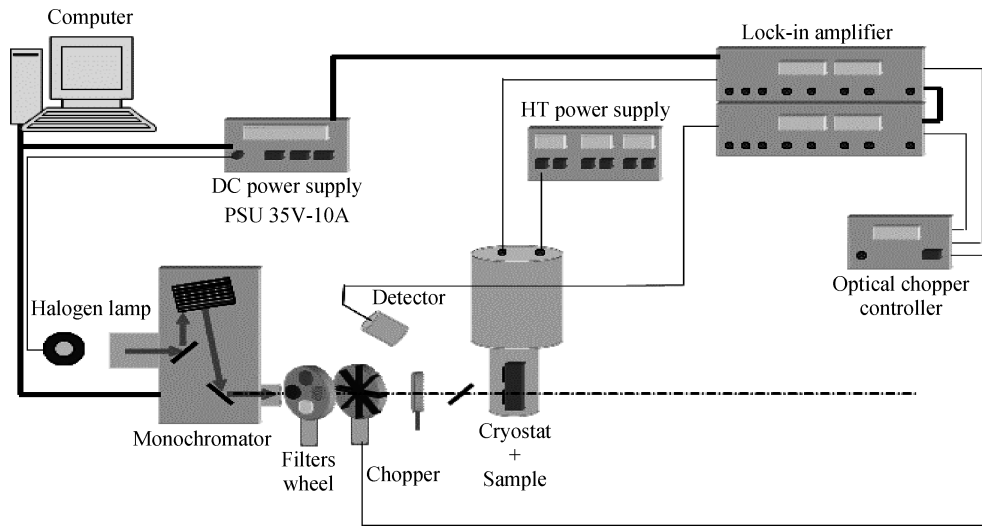


Figure 2. ac-CPM set-up.

experiment, the photon energy $h\nu$ is varied and the ac photon flux magnitude Φ_{ac} is adjusted to keep the magnitude of the ac-photoconductivity $|q(\mu_n \hat{n} + \mu_p \hat{p})|$, constant over the whole $h\nu$ range. The single transition ac absorption coefficient is then deduced as follows:

$$\alpha_{n(p)}^{ac}(E_i, h\nu, \omega) = \frac{|\hat{G}_{n(p)}(E_i, h\nu\omega)|}{\phi_{ac}} = \frac{K}{h\nu} D_{CB(VB)} |\hat{n}_t(E_i, \omega)| [D_t(E_i)]. \quad (5)$$

With \hat{n}_{ti} replaced by $\hat{D}^0, \hat{D}^+, \hat{D}^-$ for transitions from (into) dangling bond defect states, and the total absorption coefficient as:

$$\alpha_{n(p)}^{ac}(h\nu, \omega) = \sum_i \alpha_{n(p)}^{ac}(E_i, h\nu, \omega). \quad (6)$$

The DOS distribution is calculated from the absorption coefficient, after Pierz *et al.*^[10], using the derivative:

$$D(E) = \frac{1}{KD_{VB}} \left. \frac{d[h\nu\alpha_{n(p)}^{ac}(h\nu, \omega)]}{d(h\nu)} \right|_{h\nu=E_c-E}. \quad (7)$$

4. Experimental details

Microcrystalline silicon film 00c354 of thickness $d = 0.42 \mu\text{m}$ was prepared at Forschungszentrum Jülich Germany. The 00c354 film was deposited on Corning glass in a VHF PECVD system operating at 95 MHz, with a substrate temperature of 185 °C, chamber pressure of 0.3 Torr, RF power of 5 W, and gas flow ratio r equal to 3% (r represents the silane concentration: silane to hydrogen gas flow ratio $[\text{SiH}_4] / [\text{SiH}_4 + \text{H}_2]$). Electrical contacts of 1 cm length and 0.05 cm separation were deposited to form a gap cell.

The CPM experiment allows us to measure weak absorption corresponding to the deep defects. This enables us to deduce the nature and the energy distribution of the deep defects

in the gap starting from the measurement of the optical absorption coefficient. A schematic picture of the CPM experiment which has been used in this work is shown in Figure 2. A halogen lamp was used as a light source. The monochromator with a grating of 600 grooves/mm and a filter wheel were used for scanning wavelength. An optical chopper was used for measurement at frequency of 60 Hz. The light intensity was monitored and the ac-photocurrent was measured by the same lock-in amplifier. In the CPM, absorption coefficients are obtained as the inverse of the incident photon flux under constant photocurrent conditions. Absolute CPM spectra were obtained by monitoring the transmitted photon flux following the procedures described by Vanecek *et al.*^[5]. Data were then calibrated by reference to optical transmission measurements, through the use of the Ritter-Weiser formula^[16]. The DOS was obtained by differentiation of the absorption curve, as described by Pierz *et al.*^[10].

5. Results and discussion

In Figure 3, we have presented the measured absorption coefficient of the microcrystalline silicon thin film 00c354 at 60 Hz using the ac-CPM set up depicted in Figure 2.

Figure 3 shows that for values of photon energies less than 1.2 eV, the curve is viewing similarities to a defect tail because of the contribution of the amorphous phase.

By applying the derivative method of Pierz *et al.*^[10] on the measured ac- $\alpha(h\nu)$ of Figure 3, we have been able to determine the density of states distribution above the valence band edge, as illustrated in Figure 4.

It is found that the DOS have slowly decaying states for the valence band tail equals to 63 meV. Furthermore, we have developed a computer code to simulate the CPM in the case of a dynamic photo-excitation mode. The DOS distribution model for the 00c354 thin film used in our numerical modeling program of ac-CPM is compounded from three parts;

(1) For the lower part of the energy gap, above the valence band edge, the DOS distribution has a slope equal to 63 meV, as derived from the measured ac-CPM spectrum at 60 Hz.

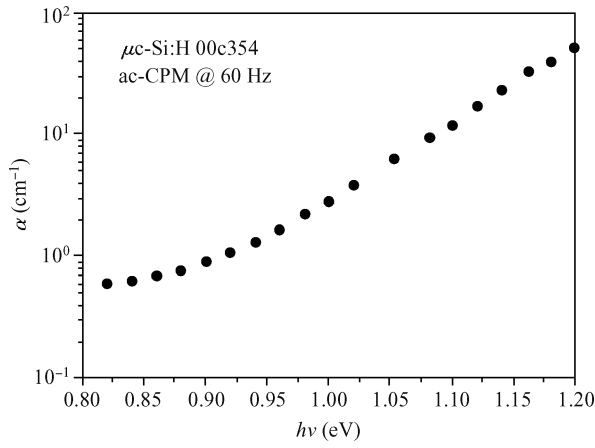


Figure 3. Absolute ac-CPM $\alpha(h\nu)$ spectrum measured at 60 Hz frequency for the 00c354 sample.

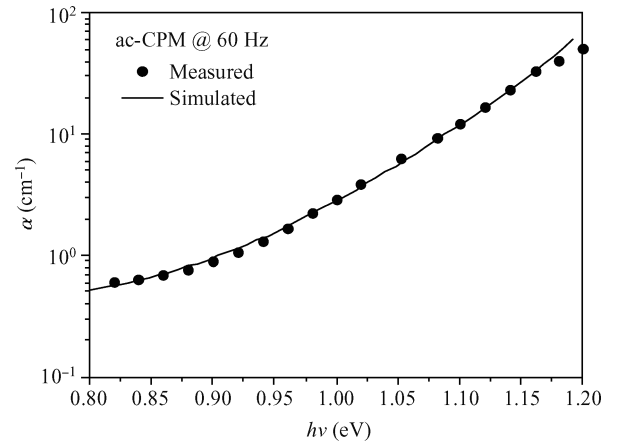


Figure 5. Measured and simulated absorption coefficients at a frequency of 60 Hz.

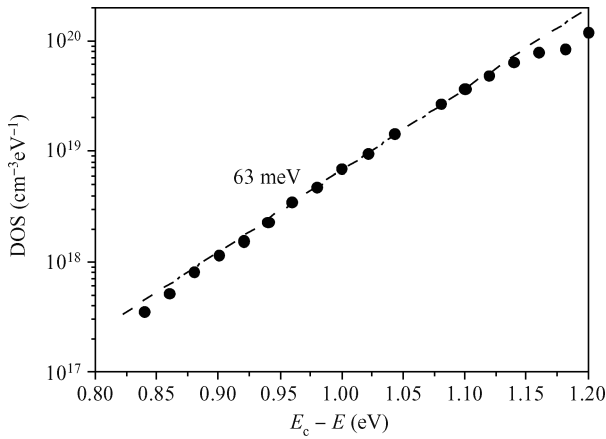


Figure 4. Extracted DOS distribution using our ac-CPM $\alpha(h\nu)$ measurements.

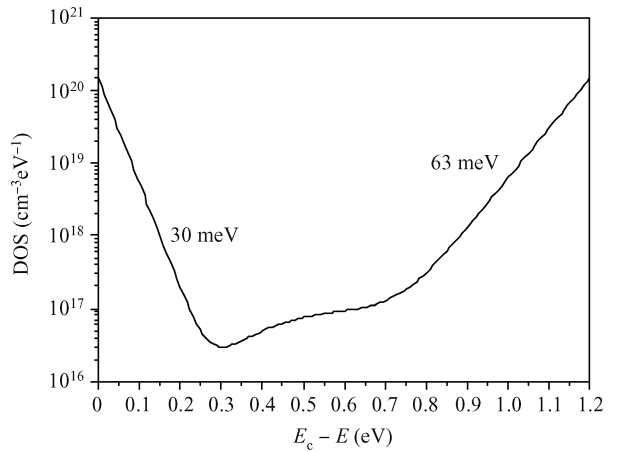


Figure 6. Derived DOS for the 00c354 sample.

(2) For the upper part of the energy gap, below the conduction band edge, the DOS distribution is derived from previous data for the same material based on transient photoconductivity. The DOS is found to have a steeper tail for the conduction band tail equal to 30 meV^[9, 11].

(3) For the middle part of the energy gap, we have completed the DOS model by choosing the appropriate parameters close to the mid-gap according to hydrogenated amorphous silicon dangling bond defect model^[12–15].

The following table summarizes the most important parameters of the μc -Si thin film 00c354.

In Figure 5 we present the measured absorption coefficient at frequency 60 Hz using our ac-CPM set up and the simulated absorption coefficient at frequency 60 Hz using our source code. The two curves are in excellent agreement.

Therefore, we can conclude that the defect states distribution is obtained and we have been able to construct complete DOS distributions over a wide range of energies of our undoped μc -Si:H thin film 00c354. The derived DOS is illustrated in Figure 6.

Table 1. Density of states parameters used for undoped μc -Si:H.

Parameter	Value
Electron mobility μ_n	$1 \text{ cm}^2 \text{ V}^{-1} \text{ s}^{-1}$
Hole mobility μ_p	$0.1 \text{ cm}^2 \text{ V}^{-1} \text{ s}^{-1}$
Density of states G_c and G_v at the mobility edges E_c, E_v	$1.5 \times 10^{20} \text{ cm}^{-3} \text{ eV}^{-1}$
Mobility gap E_g	1.2 eV
Temperature T	300 K
Inverse logarithmic slope KT_c for the CBT	0.03 eV
Inverse logarithmic slope KT_v for the VBT	0.063 eV
Total defect density N_{DB}	$1.5 \times 10^{14} \text{ cm}^{-3}$
Width of the dangling bounds distribution σ	0.15 eV
Correlation energy U	0.2 eV

6. Conclusion

In the present work, the electronic properties of μc -Si films have been studied by using ac-CPM. We have employed numerical modelling of ac-CPM to elucidate the experimental results. By analyzing the measured and simulated absorption coefficients, we have found that the density of valence band-tail

states falls exponentially towards the gap with a typical band-tail width of 63 meV. Combining the information derived from experiment study and numerical simulation, a schematic picture of the whole DOS in energetic sense has been obtained. Our study indicates that both experimental and numerical simulations of the CPM are able to extract the whole density of localized states in $\mu\text{c-Si:H}$ films.

Acknowledgments

The authors are thankful to C. Main and S. Reynolds for provision of basic ac-CPM modelling code and for fruitful discussions during a research visit to University of Dundee where the CPM experiment was done. The authors are grateful to the Algerian Ministry of Higher Education and Research for support.

References

- [1] Chen S H, Chang T W, Wang H W. Quality evaluation for microcrystalline silicon thin-film solar cells by single-layer absorption. *International Journal of Photoenergy*, 2012
- [2] Chen S H, Wang H W, Chang T W. Absorption coefficient modeling of microcrystalline silicon thin film using Maxwell-Garnett effective medium theory. *Opt Express*, 2012, 20(6): A197
- [3] Kocka J, Fejfar A, Mates T, et al. The physics and technological aspects of the transition from amorphous to microcrystalline and polycrystalline silicon. *Phys Status Solidi C*, 2004, 1(5): 1097
- [4] Larbi F, Belfedal A, Sib J, et al. Density of states in intrinsic and n/p-doped hydrogenated amorphous and microcrystalline silicon. *J Modern Phys*, 2011, 2: 1030
- [5] Vanecek M, Kocka J, Poruba A, et al. Direct measurement of the deep defect density in thin amorphous silicon films with the absolute constant photocurrent method. *J Appl Phys*, 1995, 78(10): 6203
- [6] Fejfar A, Poruba A, Vanecek M, et al. Precise measurement of the deep defects and surface states in a-Si:H films by absolute CPM. *J Non-Crystalline Solids*, 1996, 198(200): 304
- [7] Jackson W B, Amer N M, Boccara A C, et al. Photothermal deflection spectroscopy and detection. *Appl Opt*, 1981, 20(8): 1333
- [8] Lee S, Kumar S, Wronski C. A critical investigation of a-Si:H photoconductivity generated by subgap absorption of light. *J Non Crystalline Solids*, 1989, 114: 316
- [9] Brüggemann R. Numerical modelling of transient photoconductivity for density of states determination in microcrystalline silicon. *Phys Status Solidi C*, 2004, 1(5): 1227
- [10] Pierz K, Hilgenberg B, Mell H, et al. Gap-state distribution in N-type and P-type a-Si:H from optical absorption. *J Non-Crystalline Solids*, 1987, 97(98): 63
- [11] Reynolds S, Smirnov V, Main C, et al. Transient photocurrents in microcrystalline silicon films. *Proceedings of Materials Research Society*, 2002: 715
- [12] Brammer T, Stiebig. Defect density and recombination lifetime in microcrystalline silicon absorbers of highly efficient thin-film solar cells determined by numerical device simulations. *J Appl Phys*, 2003, 94(2): 1035
- [13] Meaudre M, Meaudre R, Vignoli S, et al. Density of states in hydrogenated microcrystalline silicon determined by space charge limited current. *J Non-Crystalline Solids*, 2002, 299(302): 626
- [14] Hattori K, Musa Y, Murakami N, et al. Photocarrier transport in undoped microcrystalline silicon studied by the modulated photocurrent technique. *J Appl Phys*, 2003, 94(8): 5071
- [15] Reynolds S. Carrier mobility, band tails and defects in microcrystalline silicon. *J Phys: Conference Series*, 2010, 253: 012002
- [16] Ritter D, Weiser K. Suppression of interference fringes in absorption measurements on thin films. *Opt Commun*, 1986, 57(5): 336
- [17] Schmidt J A, Rubinelli F A. Limitations of the constant photocurrent method: a comprehensive experimental and modeling study. *J Appl Phys*, 1998, 83(1): 339